# A Measurement of Anisotropy of the Cosmic Background Radiation at $1.5^o$

Todd Gaier, Jeffrey Schuster, Joshua Gundersen, Timothy Koch,
Peter Meinhold, Michael Seiffert, Philip Lubin

*Department of Physics*
*University of California*
*Santa Barbara CA 93106*

ABSTRACT: We report a recent result of a search for spatial anisotropies of the Cosmic Background Radiation. Our receiver operates with four equally spaced channels from 25-35 GHz with a beam size of $\approx 1.5^o$ FWHM. The system operated successfully for 500 hours at the South Pole during 1990-91 austral summer. The data from one region, representing 27 hours after editing, are presented here. Strong signals are present in the lower frequency channels, but with a spectrum unlike CBR fluctuations. The highest frequency channel has the smallest excess signal and can be used to set a 95% confidence level upper limit of $\frac{\Delta T}{T} \leq 1.4 \times 10^{-5}$ for fluctuations with a Gaussian autocorrelation function at a coherence angle of $1.2^o$.

*Subject headings*: cosmic background radiation - cosmology

# INTRODUCTION

Spatial anisotropies of the Cosmic Background Radiation (CBR) provide a critical test for cosmological theories. There have been no intrinsic CBR fluctuations detected to date. Current upper limits are $\frac{\Delta T}{T} \leq 1.8 \times 10^{-5}$ at arcminute scales (Readhead et.al.1988),$3.5 \times 10^{-5}$ at $0.5^o$ (Meinhold and Lubin ,1991) and $1.6 \times 10^{-5}$ at $10^o$ larger scales (Meyer et al. 1991, Smoot et. al. 1991). At a few degrees the previous upper limits are $\frac{\Delta T}{T} \leq 1 \times 10^{-4}$ (Timbie and Wilkinson,1990).

Scales of a few degrees are of special interest as they provide a probe of structures of horizon size at decoupling, as well as testing theories of structure formation with significant early reionization . CBR fluctuations of this scale arise largely via the Sachs-Wolfe effect (Sachs and Wolfe 1967) and provide a direct probe of $\frac{\delta\rho}{\rho}$ at $z_{dec}$. These results can be compared with optical data of Large Scale structure as a test of cosmological models.

Standard Cold Dark Matter (CDM) models predict structure in the CBR on scales of 1 arcminute to a few degrees, depending on the model. The angular scale increases for $z_{rec} \ll 1100$. For an ionized universe , CDM predicts significant structure on scales of 1-2 degrees at a level $\frac{\Delta T}{T} \geq 2 \times 10^{-5}$ (Bond and Efstathiou 1990?, Bond et. al. 1991). A sensitive experiment at this angular scale can further constrain the parameters of CDM.

At these sensitivities, experiments performed at any wavelength are expected to detect signals from confusing sources. These include foreground galactic emission, extragalactic discrete sources, terrestrial atmospheric signals and sidelobe pickup (Davies et. al.,Franchescini et al). As such, it has become necessary to obtain more information than monochromatic measurements of anisotropy can provide. Simultaneous measurements at several frequencies can, in principle, allow one to distinguish between intrinsic CBR fluctuations and confusing sources.

## The Experiment

The experiment used the UCSB off-axis Gregorian telescope described in previous publications (Meinhold and Lubin 1991, Meinhold et. al. 1991,submitted). The reader should refer to these papers for many of the experimental details.

The significant difference between the previous experiments and this one is the detector. We installed a broadband HEMT amplifier cooled to $\approx 6K$ in a $He^4$ cryostat. The amplifier operates from 25-35 GHz (8-12 mm) with a receiver noise temperature of about 30 K. The band was split into four 2.5 GHz bands using an array of circulators and high rejection waveguide filters. Splitting the band provides spectral information on any signals detected. A system schematic is shown in Fig. 1. Channels 1 through 4 correspond to low frequency to high frequency channels respectively. The amplifier is attached directly to a cooled scalar horn which feeds the optics. A sheet of 5-mil black polyethylene heat sunk at 77K shields the cold space from infrared radiation without effecting the bandpass of the receiver.

The optical arrangement results in a $1.65^o$ (Gaussian FWHM) measured beam at a frequency of 27.7 GHz. The beam is expected to vary as:

$$\theta_{FWHM}(\nu) = 1.65^o \times (\frac{27.7}{\nu_{GHz}})$$

The beamwidth of channel 4 is $1.35^o$. Low sidelobe response is critical in this experiment and has been measured to be less than $10^{-6}$ for angles $> 30^o$ from boresight. The beam is chopped at 8 Hz by nutating the secondary mirror with a resonant counter-rotating servo motor. The beam is thrown sinusoidally with an amplitude of $1.5^o$ on the sky. This angle is limited both by the chopper mechanism and sidelobe requirements.

The signals out of the detector diodes are fed into lock-in amplifiers with ideal integrator output filters (integration time = 1.25 s) and are then digitized. After locking in, the beams have an effective horizontal separation of $2.1^o$ on the sky. The entire telescope sits

on a rotation table which, in this configuration, points the beam to an accuracy of $< 10$ arcminutes.

The chopped noise that we expect from this system is between 1.35 and 1.6 $\frac{mK}{\sqrt{Hz}}$ $(1\sigma)$ for the different channels. When shot noise from the atmosphere and CBR are included, the noise should be between 1.6 and 2.2 $\frac{mK}{\sqrt{Hz}}$. During this run the actual noise varied between 1.8 and 4.5 $\frac{mK}{\sqrt{Hz}}$ in the lowest noise channel. We will make some attempt to address this excess above the expected noise.

## Observation Strategy

When deciding upon an observation strategy several factors were considered. As much integration time as possible was desired at each point on the sky, but also enough points were required to provide sufficient degrees of freedom for the final statistical analysis. In addition, foreground galactic contamination, solar sidelobe pickup, atmospheric noise, and system $\frac{1}{f}$ were be taken into account.

A discrete scan strategy similar to previous work (Meinhold and Lubin,1991) was adopted. This scan consists of moving the telescope in azimuth by $2.1^o$ steps on the sky in order to overlap the chopped beams. This technique takes advantage of the topographic location of the South Pole, to track in RA without changing elevation. This minimizes possible atmospheric or gravitational offsets, as well as eliminating the problem of beam rotation.

An N point scan will sample a region $2.1^o \times (N+1)$ across the sky. We examined a low frequency (408 MHz) map (Haslam et al.) and the IRAS 100 $\mu$ map to determine a nominal scan size and location that would be relatively free from galactic synchrotron and dust emission. Simulations of the instrument response on this map showed that typical signals of $20\mu K$ (RMS) would be seen at 30 GHz over a $20^o$ scan. For scans larger than

this, significantly larger galactic signals are expected.

For all of these reasons, a 9 point scan was chosen. Because of the galactic contamination problem, we felt it would be desirable to build a 2-d map of the region. The map consists of 6 scans of 9-points separated in elevation by $0.75^o$, centered at $\alpha = 0.5hr$, $\delta = -62.25^o$. The sun was at an angle $\geq 68^o$ in azimuth from the edge of the map for the duration of the observation. In addition we ran a deep 13 point scan and a 15 point scan overlapping the map region. To test the system sensitivity to small signals, a galactic plane crossing and a 9 point scan of the Large Magellanic Cloud (LMC) were performed.

The system was calibrated one or two times a day by inserting a warm target into the beam. The calibration in channel 1 varied by $\pm$ 5.5%($1\sigma$) during the measurement period, while the variation in channels 1-3 was less than $\pm$ 3.2% . The calibration and beam were also tested by detailed scans of the moon.

The instrument collected data for a total of about 500 hours during the 1990-91 South Pole summer. After editing for weather and system faults, about 150 hours remain. The data presented here are from a 9 point scan at the center of the map($\delta = -62.25^o$). This scan had the longest total integration time and was expected to be relatively free from galactic contamination. This data represents 100 hours of total data and 27 hours of edited data. The remainder of the data will be presented at a later date.

## Data Editing and Reduction

The data were edited in the following fashion. First we removed outliers in the raw data (points deviating by $> 5\sigma$ in a 20 second sample). This removed less than 1% of the total data. The data were then binned into scan positions of constant RA, eliminating points between scan positions. The finite slew rate of the telescope resulted in a 90% scan efficiency.

The large chop angle on the sky pushed the chopper mechanism to its mechanical limits. Occasionally, the chopper became unstable or varied in amplitude. This had the effect of distorting the beam on the sky and possibly changing the reference signal to the lock-in amplifiers. For this reason the chopper was monitored and when the amplitude or zero position fell outside a specified range, all data were removed.

The single largest source of data loss was bad weather. Even though the South Pole has been proven to be an excellent observation site with exceptionally low precipitable $H_2O$ content (Fig. 2)†, at times of cloudy skies the noise could increase by a factor of 10. The criteria for removal of noisy data was determined for each channel individually, as the RMS above which the data fail to integrate down. These values are 3.57, 3.1, 4.0 and 3.7 $\frac{mK}{\sqrt{Hz}}$ for channels 1 to 4 respectively. 70% of the data from the 4 days of observation were removed this way.

We define a full scan as starting at position 1 and ending at position 1. A half scan starts at position 1 and ends at position 9. The raw data at each point is of the approximate form:

$$\Delta_i = T_{\gamma_i + c/2} - T_{\gamma_i - c/2}$$

the usual single difference form, with c as the chop angle $2.1^o$. $T_{\gamma_i}$ is the CBR temperature at angle $\gamma_i$, convolved with our beam, which in the gaussian approximation is given by; ‡

$$\sigma_b = \theta_{FWHM}(\nu) \times 0.4247$$

The data were divided into half scans and a line was fit to the data as a function of time in each half scan. This had the effect of removing a line in RA from the final data

† The atmospheric water content was typically 1 mm during the observation period, growing as high as 3 mm during inclement weather

‡ Effective $\sigma_b$ is actually larger in one dimension due to the sinusoidal chop.

set. The resulting approximate form of the data is

$$\Delta_i' = \Delta_i - (\gamma_i m + b)$$

The values m and b are the slope and offset given by a least squares fit to the data $\Delta_i$. The removal of the line only effects our sensitivity at angular scales large compared to our beam. The typical size of the removed signal was $\approx 250\mu K$ (as high as 800 $\mu K$) between points 1 and 9, and is not spectrally variant. Partial half scans were totally removed. An error window was defined for elevation of $\pm 7.2'$ (the elevation was not servoed to correct for wind). The data were then binned into RA and an average and standard deviation were calculated. This data from all four channels is displayed in Fig. 3. The units are $\mu K$ thermodynamic and the error bars are $\pm 1\sigma$.

## Data Analysis

Prior to binning, the data between channels are partially correlated. A sample correlation scatter plot between channels 1 and 2 is shown in Fig.4. The correlation coefficient for this data $\rho = 0.29$. Such correlations are expected as all channels are observing through the same slice of atmosphere simultaneously. The correlation matrix for the entire scan is shown in Table 1. This matrix only includes data sampled simultaneously in all four channels. Not all of the data that went into the data in Fig. 3. were sampled simultaneously. This fraction of the data is intrinsically uncorrelated, resulting in the dilution of effective correlations in the final data.

Time series analysis has been performed on the components of this matrix. The magnitude of the off diagonal terms (both absolute and relative) was found to vary significantly with time. There was no significant variation of these terms as a function of scan position.

The correlated component is the right size to explain the excess noise in the data, arising from chopped atmospheric signals. The final data sets are expected to have structure which looks similar. If atmospheric fluctuations are random in time, no net signal results and the data in the four channels will appear correlated but explained by the errors. The short term correlations are being explored more deeply, but for analysis of a single channel, the effect is unimportant. They are important, however, in any spectral analysis of the data and the determination of the ultimate sensitivity of this experiment as dictated by the atmosphere.

An obvious feature of the data in Fig.3. is the large correlated signal in channels 1 and 2. The weighted covariance matrix for this binned data is shown in Table 2. The corresponding correlation matrix is shown in Table 3 for comparison with Table 1. The signal also drops sharply as a function of frequency. Considerable spectral analysis has been done on this data. A model where the most probable signals have a CBR spectrum (for Gaussian fluctuations at $1.2^o$) , is accepted with 2% probability. Similarly, a synchrotron type spectrum (antenna temperature spectral index, $\beta = -2.85$(Lawson et.al,1987, Reich and Reich,1988) is accepted with 8% probability. No assumptions are made about the angular nature of the synchrotron fluctuations, which could severely effect this result. A combination of nonlinear fitting and Monte-Carlo simulations has been used to obtain these results. The method used will be published at a later date.

The final striking feature of the data is the lack of signal in Channel 4. For the reasons outlined above, we shall assume that Channels 1,2 and 3 are dominated by foreground contamination (most probably galactic) and only use Channel 4 as a true measure of CBR signals. This assumption is conservative and can only result in weaker upper limits for most models.

A Monte Carlo analysis similar to that used previously (Meinhold and Lubin,1991) was employed in order to set upper limits to CBR fluctuations using only channel 4. CBR

fluctuations are characterized by their autocorrelation function (ACF)

$$\left\langle \frac{T_{\gamma_i}}{T_o} \frac{T_{\gamma_j}}{T_o} \right\rangle = C(\Theta)$$

where $\gamma_j - \gamma_i = \Theta$. We determined 95% confidence level upper limits to CBR fluctuations with a Gaussian ACF,

$$C(\Theta) = C_o e^{-\left(\frac{\Theta^2}{2\Theta_c^2}\right)}.$$

3000 random maps were generated with the above ACF for each value of $\Theta_c$ tested. The RMS of the assumed sky fluctuations ,$\sqrt{C_o}$ was varied, and the full experimental response simulated on each sky. Any linear trend in the data was removed, and a statistic was employed to set an upper limit. We found this upper limit to be $\langle(\frac{\Delta T}{T_o})^2\rangle^{\frac{1}{2}} = \sqrt{C_o} \leq 1.4 \times 10^{-5}$ at $\Theta_c = 1.2^o$. The power of the test was 40% and we assume $T_o = 2.735K$ (Mather et. al., 1991). The results over a broader range of angles are summarized in Fig.5.

Additionally, we performed likelihood analysis on the data using the full form of the correlation matrix, including off diagonal terms (Vittorio et. al., 1991). This form of the likelihood function is given by

$$L(C_o, \Theta_c) \equiv (2\pi)^{-N/2} |M|^{-1/2} \exp[-\frac{1}{2} \sum_{i=1}^{N} \sum_{j=1}^{N} \Delta_i' M_{ij}^{-1} \Delta_j']$$

The need for extensive simulations is eliminated by writing the theoretical correlation matrix,$M(C_o, \Theta_c)$ † in terms of theoretical data, $\langle \Delta_i' \Delta_j' \rangle$, instead of $\langle \Delta_i \Delta_j \rangle$. So

$$M_{ij} = \langle \Delta_i' \Delta_j' \rangle_{th} + \delta_{ij} \sigma_i$$

† The usual form $\langle \Delta^2 \rangle = 2T_o^2(C(0) - 2C(c))$, needs modification due to the overlapping beams in the scan strategy.

$\langle \Delta_i' \Delta_j' \rangle_{th}$ is derived using $\langle T_{\gamma_i} T_{\gamma_j} \rangle_{th} = T_o^2 C(\Theta, \Theta_c, C_o, \sigma_b)$, the beam convolved correlation function with $\gamma_j - \gamma_i = \alpha$ The actual upper limits are set using the integrated area under the resulting likelihood curve. This result is also displayed in Fig.5. The agreement between the two techniques is good.

For comparison, the reduced $\chi^2$ of this data is 0.8 with $\nu$ =7 degrees of freedom. Unless $\chi^2$ of the data is small , most statistical techniques will result in the same upper limit (Lawrence et.al. 1988).

This result represents a factor of 8 improvement over previous limits to anisotropy of the CBR at $1.2^o$ (Timbie and Wilkinson,1990). At smaller angular scales, the limits are slightly better than the previous upper limit of Meinhold and Lubin at $\Theta_c = 0.5^o$. At larger angular scales the sensitivity drops rapidly with increasing $\Theta_c$. At $4^o$ this work puts pressure on the previous detection of Davies et.al..but does not rule out such a fluctuation at the 95% confidence level. At still larger scales, the previous upper limits (Meyer et. al.,1991) are uneffected. It is interesting to note however, that the combined results of OVRO (Lawrence et. al.) at a few arcminutes, Meinhold and Lubin at tens of arcminutes,this work, and the result of Meyer et.al., constrain the entire angular range from 1 arcminute to $20^o$ to $\frac{\Delta T}{T} \leq 4 \times 10^{-5}$.

## Conclusion

We have made a sensitive map of anisotropy of the CBR at multiple frequencies. One elevation from this map, the most sensitive, has been analyzed. The lower frequencies have strong detections present, while the higher frequencies do not. This type of a spectrum is not indicative of CBR fluctuations. The data in Channel 4 (32.5-35 GHz) implies a 95% confidence level upper limit of $\frac{\Delta T}{T} \leq 1.4 \times 10^{-5}$ for Gaussian fluctuations. This represents a factor of 8 improvement over previous limits at the angular scale $\Theta_c = 1.2^o$. Work

is proceeding on the analysis of the entire map region as well as the larger scans. The ultimate sensitivity of the the entire data set should be $\frac{\Delta T}{T} \leq 8 \times 10^{-6}$. In addition we are working in collaboration with others to determine upper limits to fluctuations with an autocorrelation function consistent with current CDM models. Large scale redshift surveys (Geller et al., Faber et. al.) imply minimum CBR anisotropies (via the Sachs-Wolfe effect, Bertschinger et. al.) of $\frac{\Delta T}{T} \geq 1 \times 10^{-5}$. Signals can be larger than this if velocity field Doppler anisotropies are included. This data puts pressure on standard cosmological models to explain this discrepancy.

We would like to thank the UCSB Physics Dept. machine shop for their willingness to work tirelessly on short notice. Geoff Cook designed and built the chopper electronics. This project would not have been possible without the support and encouragement of Bernard Sadoulet. The remarkable HEMT amplifiers were supplied by Mike Balister and Marian Pospiezalski at the Low Noise Amplifier group at NRAO. This work was supported by the National Aeronautics and Space Administration, under grant NAGW-1062, and the National Science Foundation under Polar grant DPP???-????? and the Center for Particle Astrophysics under grant NSF??????. Lyman Page provided helpful comments at the South Pole and later. Finally we would again like to thank Bill Coughran and the entire ASA support staff for their support at the South Pole during the 1990-91 austral summer.

## Figure Captions

Fig. 1 Receiver schematic. This includes RF components from the feed horn to the detector diodes. Not included are isolators at the output of the four final bandpass filters.

Fig. 2 1990-91 South Pole Precipitable Water. Relative humidity as a function of altitiude measured by radio-sondes, is converted to a total column content. Day 1 refers to November 1,1990. Data from Nov 10-14 is incomplete.

Fig. 3 The binned data. Channel 1 refers to the band 25-27.5 GHz. Channel 4 refers to 32.5-35 GHz. A linear component has been removed in scan position. Scan positions are separated by $2.1^o$ on the sky. The data are in units of $\mu K$ *thermodynamic*. The error bars displayed are $\pm 1\sigma$.

Fig. 4 Correlation Plot. The 1.2 second sampled data is shown for Channel 1 vs. Channel 2. 2500 data points are displayed. The data have been edited and fit over 1/2 scans as described in the text. Data from all bins are included.

Fig. 5 Upper limits to the RMS amplitude of CBR fluctuations assuming a Gaussian ACF, calculated from the data of Channel 4 in Figure 3. The $*$ are the 95% confidence level limits found using a Monte-Carlo technique similar to that of Meinhold and Lubin. The solid line are the limits found by a Bayesian technique using the full likelihood function, including off diagonal terms in the correlation matrix.

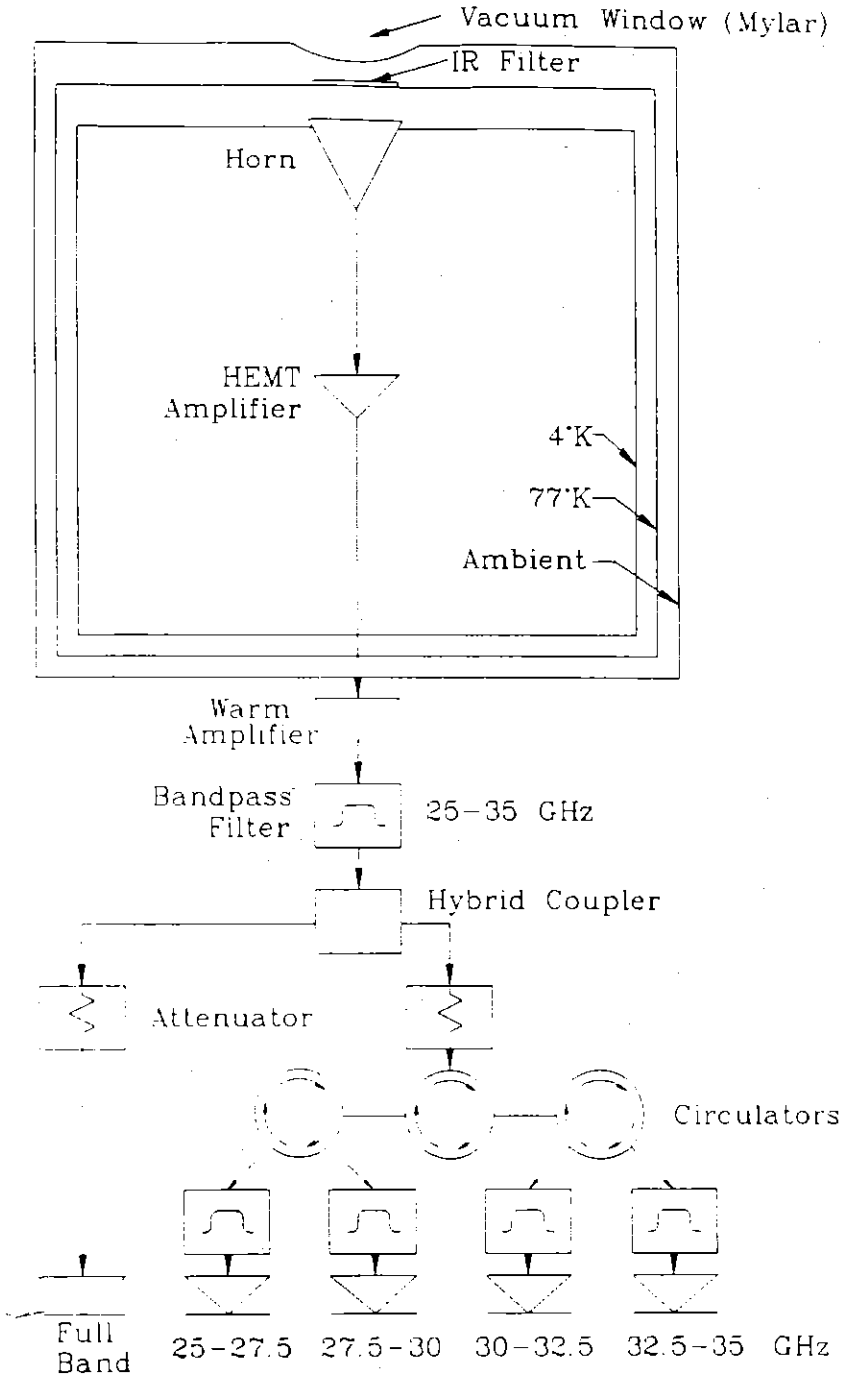
Vacuum Window (Mylar)
IR Filter
Horn
HEMT
Amplifier
4°K
77°K
Ambient
Warm
Amplifier
Bandpass
Filter
25-35 GHz
Hybrid Coupler
Attenuator
Circulators
Full
Band
25-27.5
27.5-30
30-32.5
32.5-35
GHz

Figure 1.

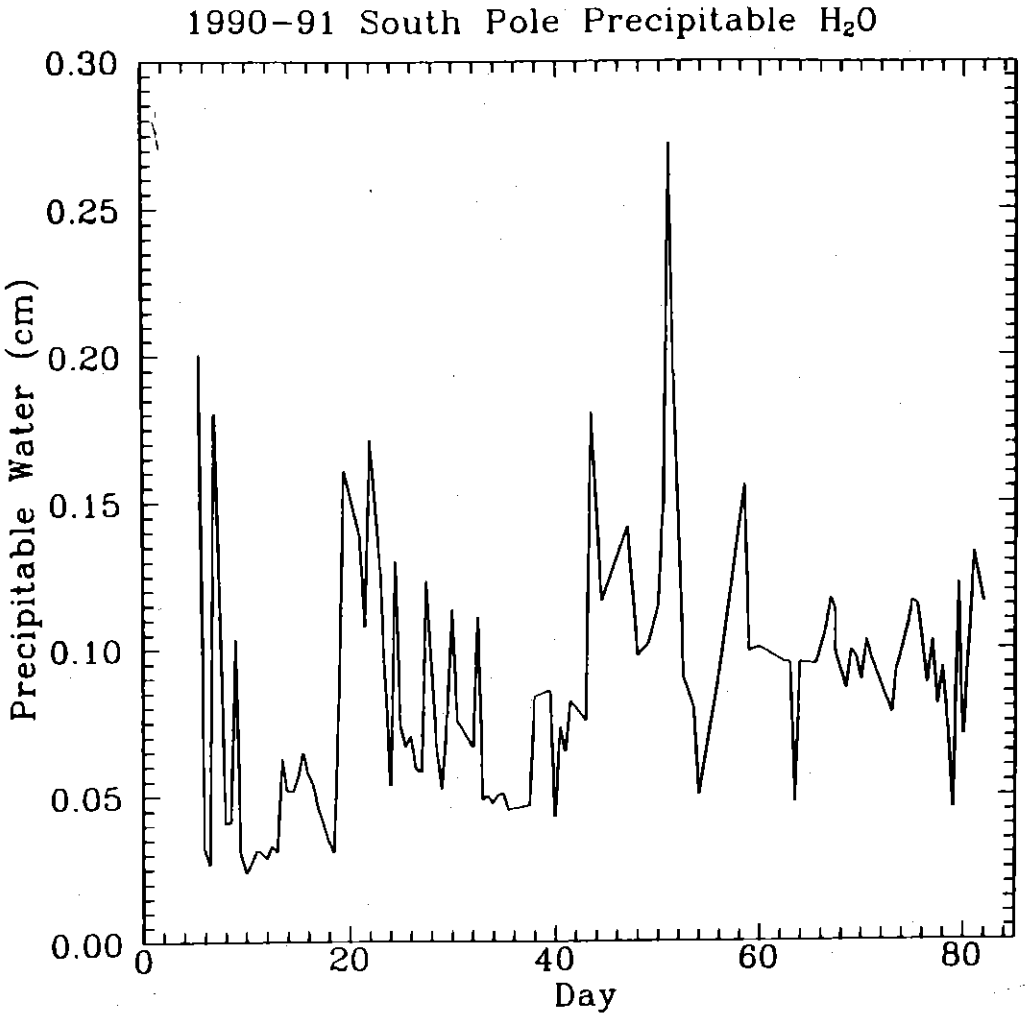
1990–91 South Pole Precipitable $H_2O$
Precipitable Water (cm)
0.30
0.25
0.20
0.15
0.10
0.05
0.00
0
20
40
60
80
Day

Figure 2.

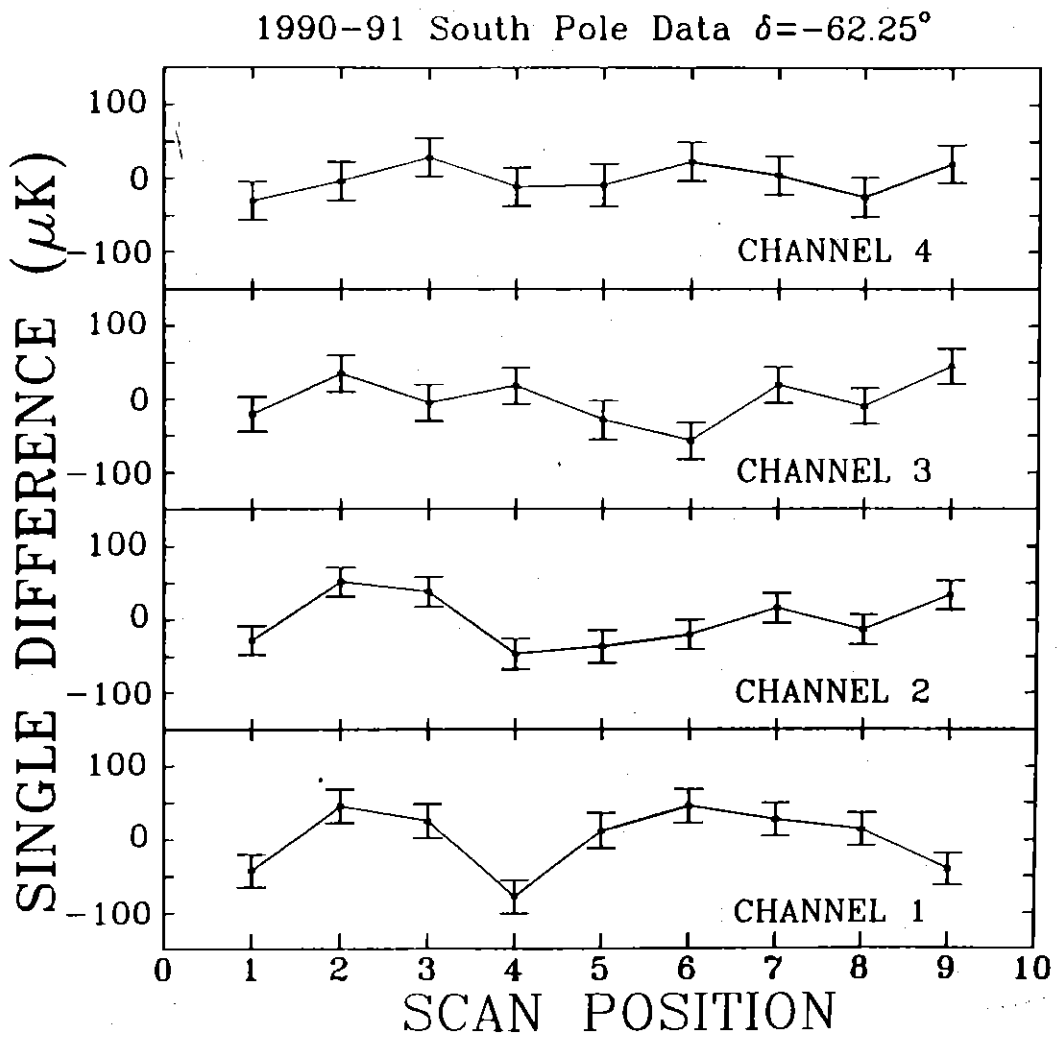
1990–91 South Pole Data δ=−62.25°
SINGLE DIFFERENCE (μK)
100
0
−100
CHANNEL 4
CHANNEL 3
CHANNEL 2
CHANNEL 1
0
1
2
3
4
5
6
7
8
9
10
SCAN POSITION

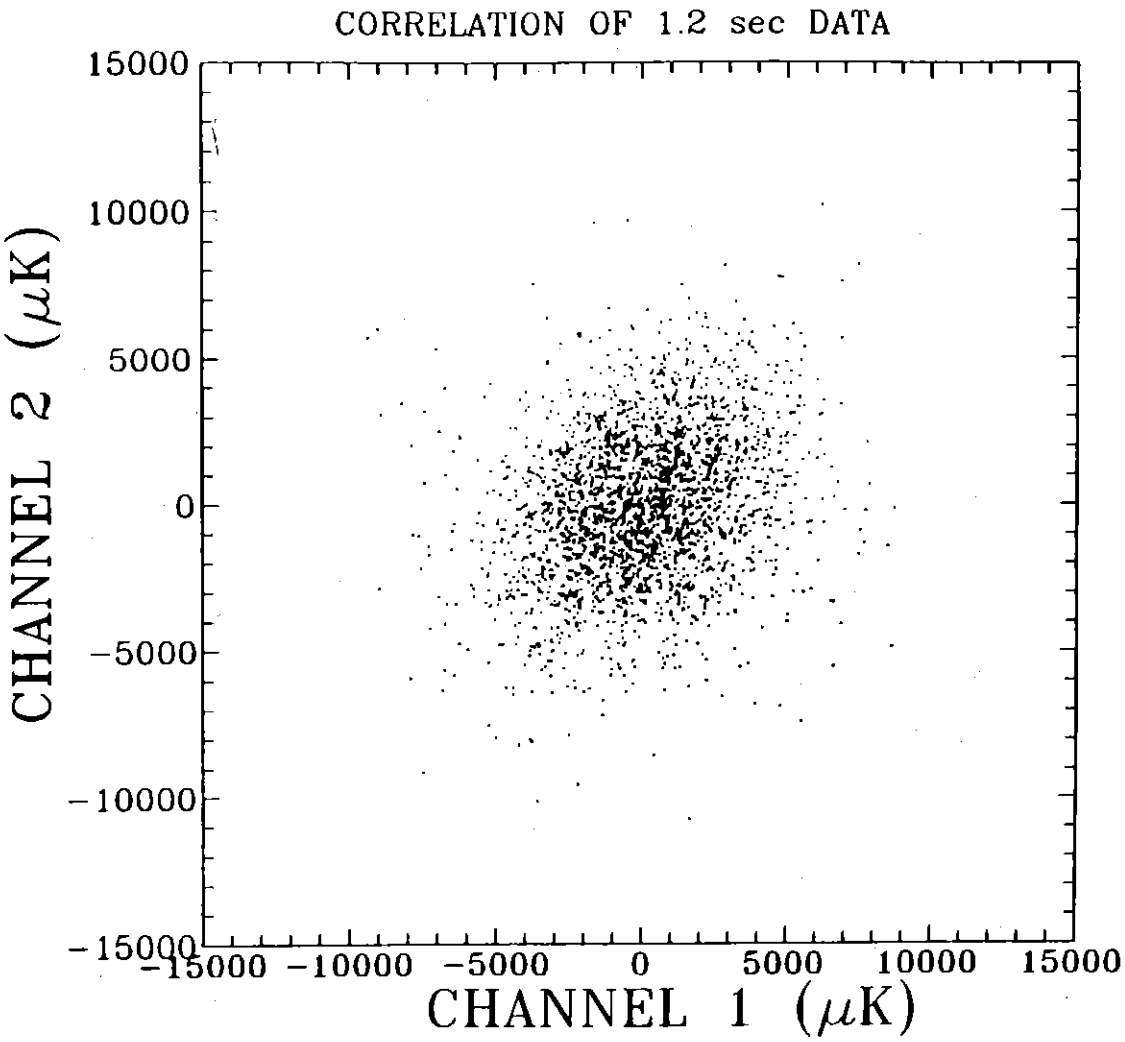
CORRELATION OF 1.2 sec DATA
15000
10000
5000
0
−5000
−10000
−15000
CHANNEL 2 (μK)
−15000 −10000 −5000 0 5000 10000 15000
CHANNEL 1 (μK)

Figure 4.

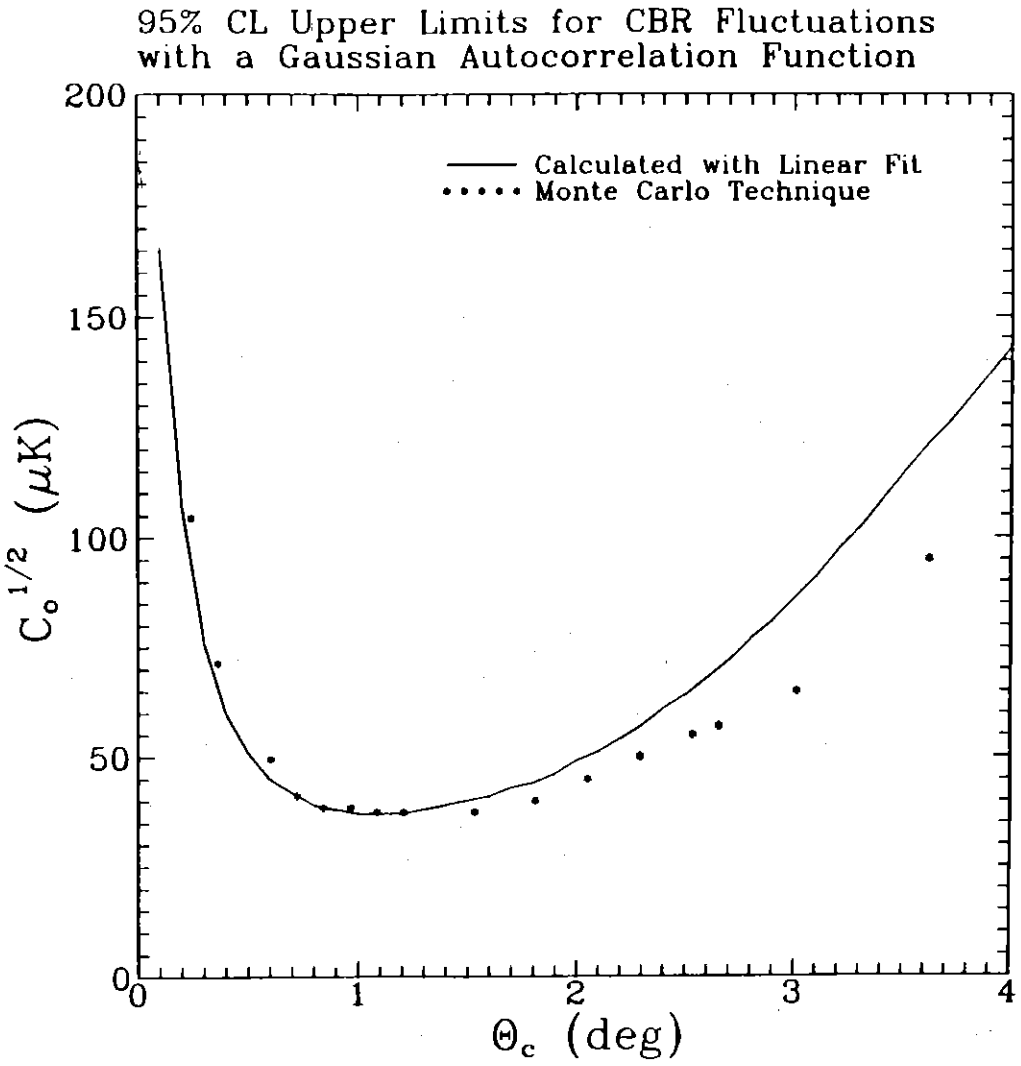
95% CL Upper Limits for CBR Fluctuations
with a Gaussian Autocorrelation Function
Calculated with Linear Fit
Monte Carlo Technique
200
150
100
50
0
0
1
2
3
4
$C_o^{1/2}$ ($\mu$K)
$\Theta_c$ (deg)

Figure 5.